SUPPLEMENTARY MATERIALS

A. General modelling framework

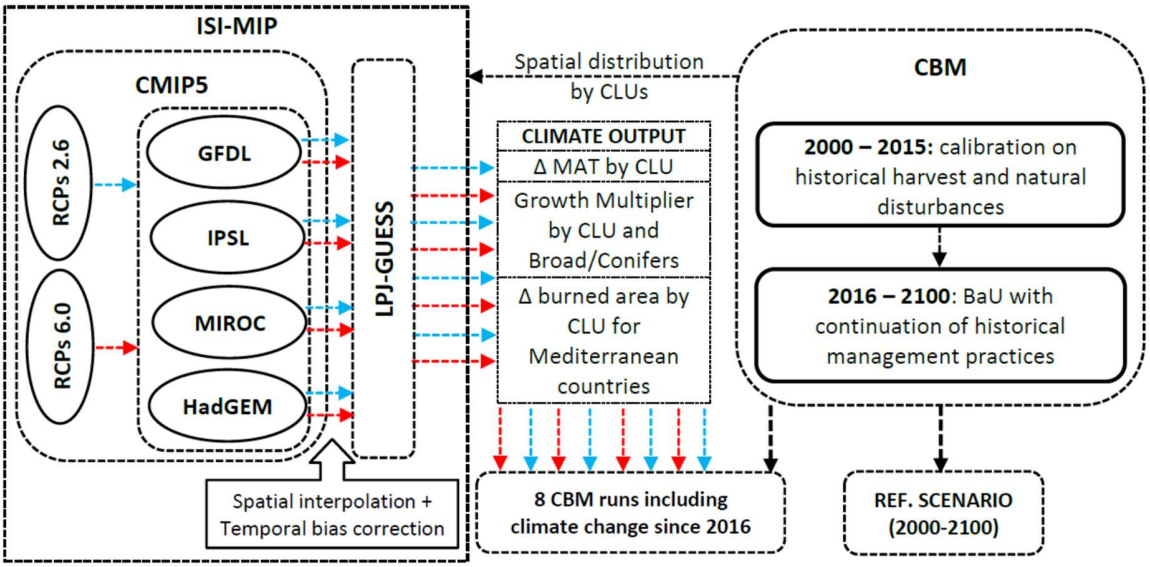

Fig. 1S: general modelling framework including the four climate models (GFDL, IPSL, MIROC, HadGEM), the Lund-Potsdam-Jena General Ecosystem Simulator dynamical global vegetation model (LP-GUESSJ) and the Carbon Budget Model (CBM).

B. Customization of the Carbon Budget Model

The Carbon Budget Model (CBM) is an inventory-based, yield-data driven model that simulates the stand- and landscape-level C dynamics of above- and belowground biomass, dead wood, litter and soil (Kurz et al., 2009). The CBM spatial framework conceptually follows the IPCC Reporting Method 1 in which the spatial units (SPUs) are defined by their geographic boundaries. Each forest stand is attributed to a SPU, characterized by age, area, and 6 classifiers, including administrative (defined at country or regional level) and ecological information (defined from Climatic Units, CLUs – see also Pilli et al., 2018), the link to the appropriate yield curves, and other parameters defining the forest types (FTs, based on the leading species), management strategy (MS, i.e., high-forests, coppices, etc.) and other management information (i.e., even-aged or uneven-aged structure).

During the model run, a library of yield tables (YTs) defines the gross merchantable volume production by age class, for each species. These yields represent the volume in the absence of

natural disturbances and management practices. Species-specific, stand-level equations convert the merchantable volume production into different aboveground biomass components (Boudewyn et al., 2007). The belowground biomass, its increment and annual turnover are calculated using the equations provided by Li et al. (2003). Annual dead wood and foliage input is estimated as a percentage (i.e., turnover rate) applied to the standing biomass stock.

To estimate the decomposition rate of each Dead Organic Matter (DOM) pool the CBM adjusts the base decomposition rates, defined at 10^{o}C, according to the mean annual temperature (MAT) defined for each SPU. Each SPU is linked to a CLU through the information provided by Corine Land Cover (see Pilli et al., 2012). Each CLU was defined by combining total monthly precipitation values collected by Hijmans et al. (2005) – assumed as constant within the present study since they do not directly affect the decomposition rate - with MAT values derived from each climate models (IPSL-CM5, GFDL, HadGEM2, MIROC 5.2). These last values were assumed as constant within the time interval 2000 -2015 (equal to the average of the MATs' values of the historical period as considered from each climate model) and as varying - compared to the average of the historical period - on annual bases since 2016 onward.

The model uses an initialization process to estimate the size of all DOM pools at the start of the simulation. The initialization starts with all DOM pools containing zero C stocks and then the model simulates multiple iterations of growth and stand-replacing disturbances, gradually increasing the size of the DOM pools. The rotations continue until the slowly-decaying C pools (i.e., the soil) at the end of two successive rotations meet a difference tolerance of 0.1% (see Kurz et al., 2009 for further details). In this study, during this preliminary stage, we apply an historical YTs library, specifically defined for the initialization, and derived from the standing volumes per age class reported by original data sources (i.e., National Forest Inventories, NFIs, or Forest management Plans, or other ancillary data). These values represent the impacts of growth and partial disturbances during stand development.

During the following run, we use a second library of YTs (named current YTs) which represent the stand-level volume accumulation in the absence of natural disturbances and management practices. Because this library is based on the current annual increment reported by countries' NFIs and other data sources (see Pilli et al., 2013, 2016), the age span covered by these growth

curves matches (at least for even-aged forests) the current age structure of each country, which is mostly the result of past management practices. In this specific study, however, with such a long model-run, the current age structure can get considerably older because, assuming the continuation of the current management practices applied within the historical period 2000 – 2015, part of the forest area will not be rejuvenated. For this reason, assuming that Y_t is the maximum age class reported from country's data for a certain FT and MT (with an age class span of 10 years), each current YT was derived from the CAI values reported from the country, until an age class equal to Y_{t+2} (i.e., 20 years older that the maximum value reported from the country - in this way the YT may directly reflect, within a short time interval, the current evolution of each FT, as determined from the past management practices). The lack of data beyond this threshold can be overcome using large datasets, including the long-term evolution of gross and net primary productivity (i.e., GPP and NPP) in aging forests. Using a global database of GPP and NPP obtained from eddy covariance measurements, Tang et al. (2014) fitted the NPP against the forest age through a gamma function applied to boreal and temperate forests. Using these parameters, we derived the relative variation of the NPP versus age for boreal and temperate forests (also used for Mediterranean countries). The same rate (reported on Fig. 2S) was applied to the annual increment estimated by the country data, starting from the age class Y_{t+2}, and until an age class corresponding to 300 years old.

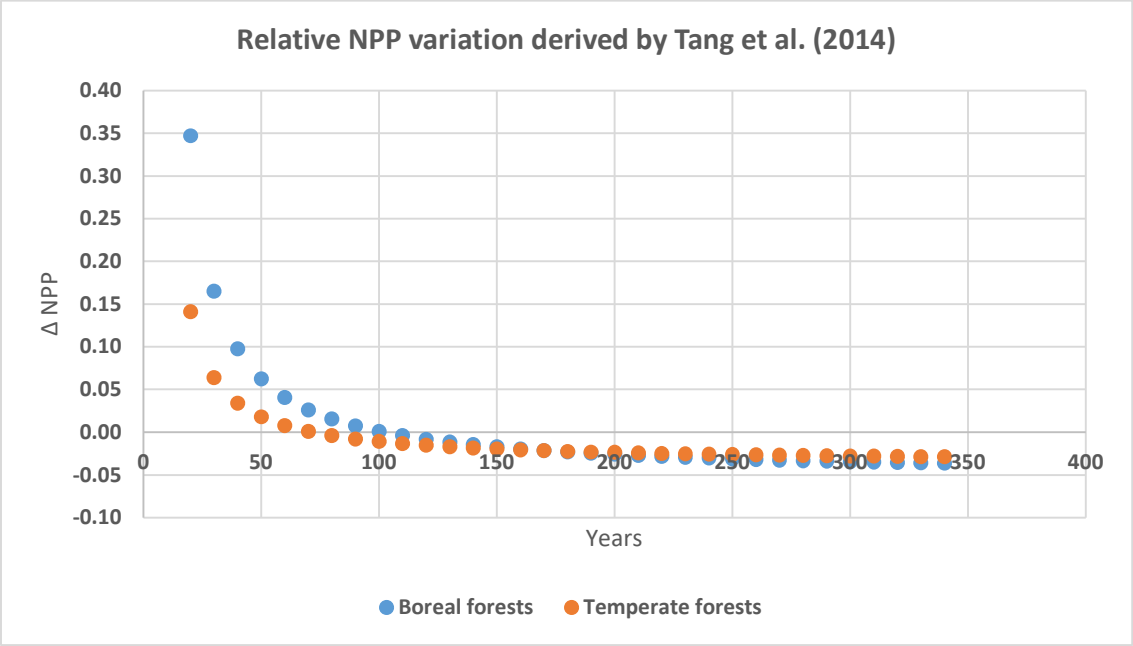

Fig. 2S: relative variation of Net Primary Production (NPP) derived from the gamma functions reported by Tang et al. (2014), further distinguished between boreal and temperate forests.

The final evolution of current annual increment against time (CAI_t) until 300 yrs., was estimated, for each country, FT and MT, using the following combined exponential and power function (Sit, 1994):

$$CAI_t = at^b c^t \qquad \text{Eq. (1)}$$

Where t is the average age reported by original data sources (e.g., NFI) for each age class, the parameter a controls the maximum increment reached by CAI and parameters b and c (assuming for our study $b>0$ and $0 \leq c \leq 1$, according with the values proposed by Sit, 1994) control the shape of the curve. Parameters were estimated using the Marquardt method (Motulsky and Ransnas, 1987) provided by the SAS® software. Further methodological details are reported in Pilli et al., 2013.

Since the evolution of increment of uneven-aged forests was already based on an exponential function with the same pattern reported in Fig. 2S (see also Pilli et al., 2013, App. C), no further correction was applied to estimate the long-term evolution of this management system.

Because all inventory data currently used by CBM are referred to the period 1992 – 2015 (see the Annex in Grassi and Pilli, 2017), we assume that the default values provided by the current

YTs represent the average, current gross volume increment of each stand (Pilli et al., 2013) during the historical period 2000 – 2015. The values reported by the YTs define the gross merchantable volume of the main stem and the annual difference between these values is the net annual increment before losses from disturbances (Kull et al., 2016). During the model run, CBM applies a set of natural and anthropogenic disturbances such as fire, windstorms and partial or clear-cut harvesting, defined by the user, but the model does not simulate the impacts of climate changes on forest growth and on heterotrophic respiration (Kurz et al., 2009). On the opposite, climate models estimate the impact of climate changes, including annual variations of MAT and total annual precipitation, on forest growth and heterotrophic respiration, excluding the impact of anthropogenic disturbances. We derived from these models a set of growth multipliers (GMs, further distinguished between broadleaves and conifers and scaled at CLU level), proportional to the relative variation of the biomass stock as estimated from climate model under each RCPs. Within the CBM run, these GMs were applied, starting from 2016, to the current YT library as defined above, varying the relative net growth of each FT, according to the impact of climatic conditions, as considered from each process-based model.

C. Supplementary materials on input data

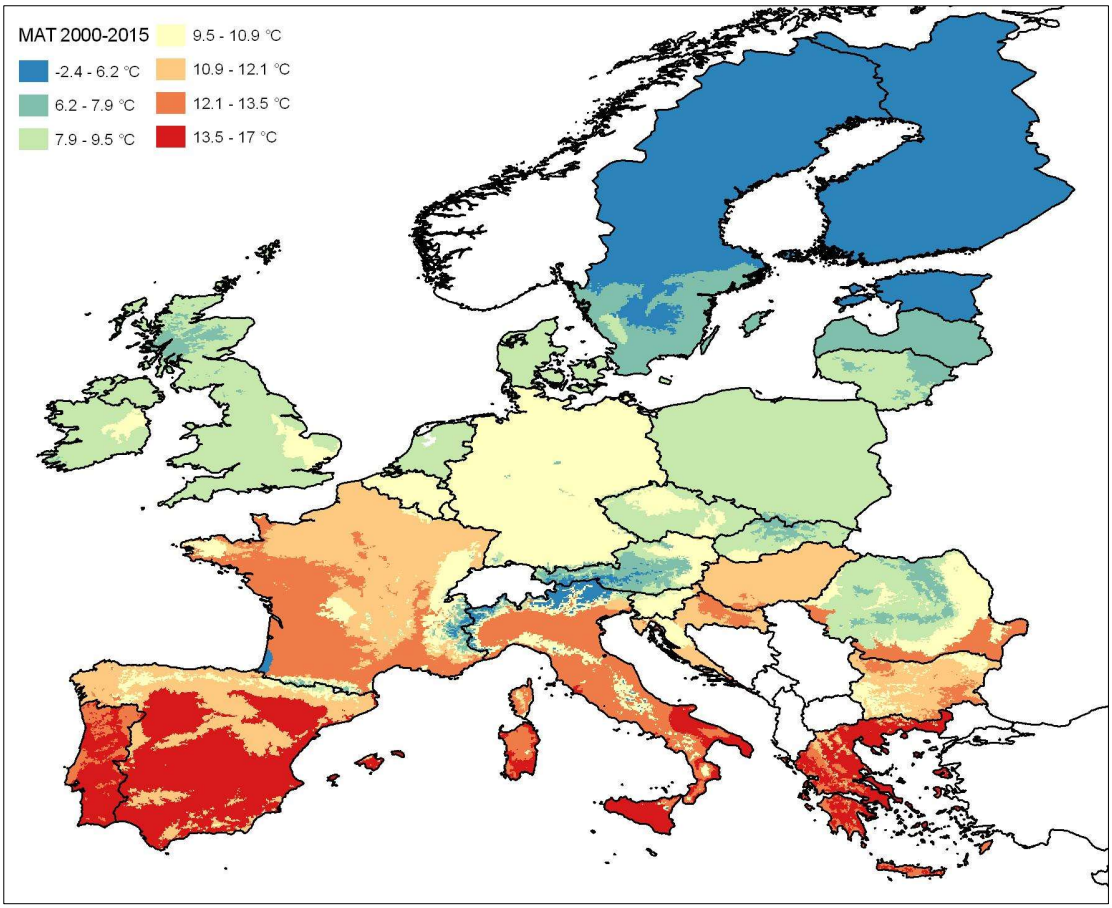

Fig. 3S: mean annual temperature data as defined from climatic models and used as input for CBM for the historical period 2000 – 2015, further scaled at CLU level.

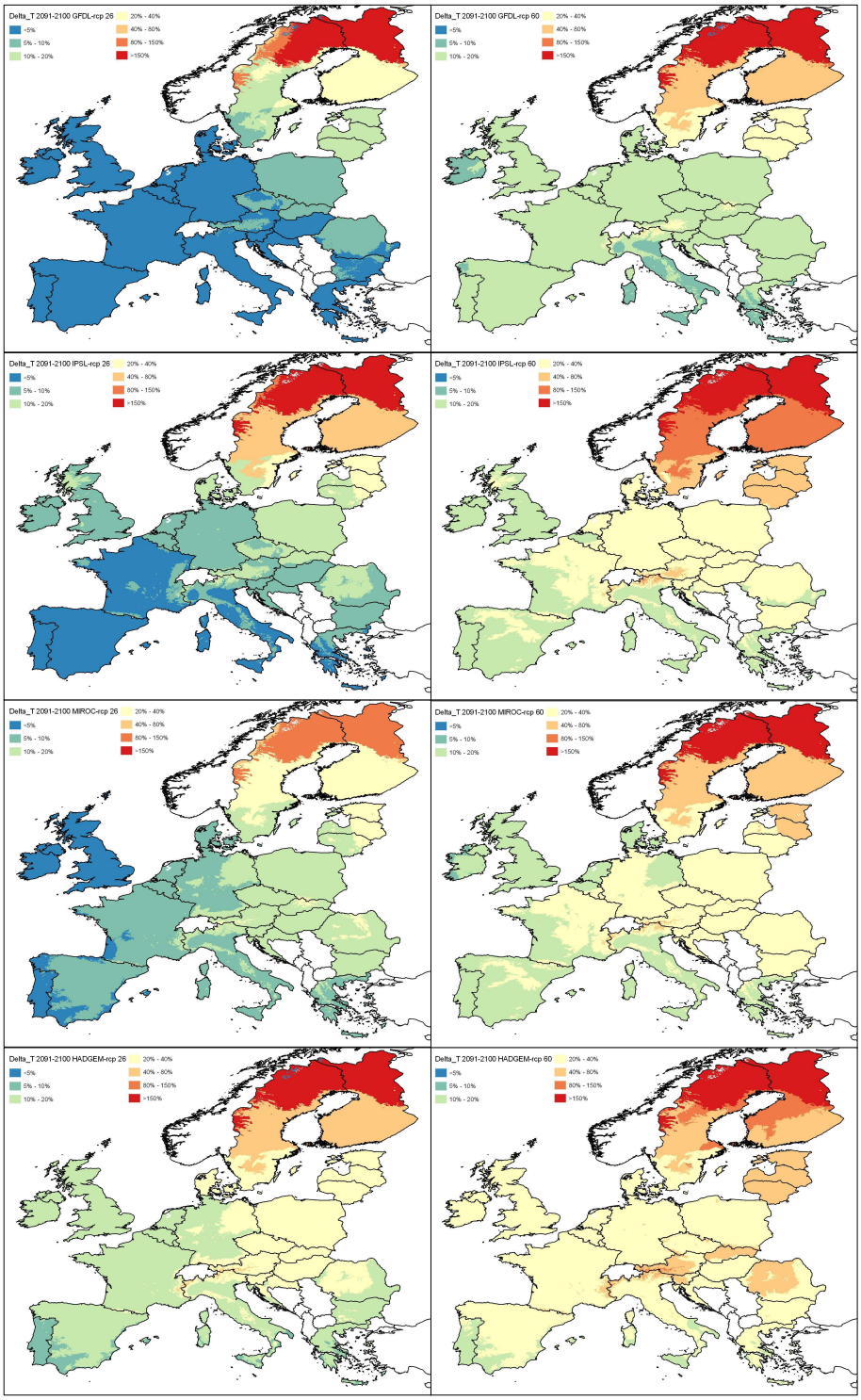

Fig. 4S: relative variation of Mean Annual Temperature data as estimated from climatic models within the period 2016 - 2100. RCP 26 is reported on the left side and RCP 60 on the right side

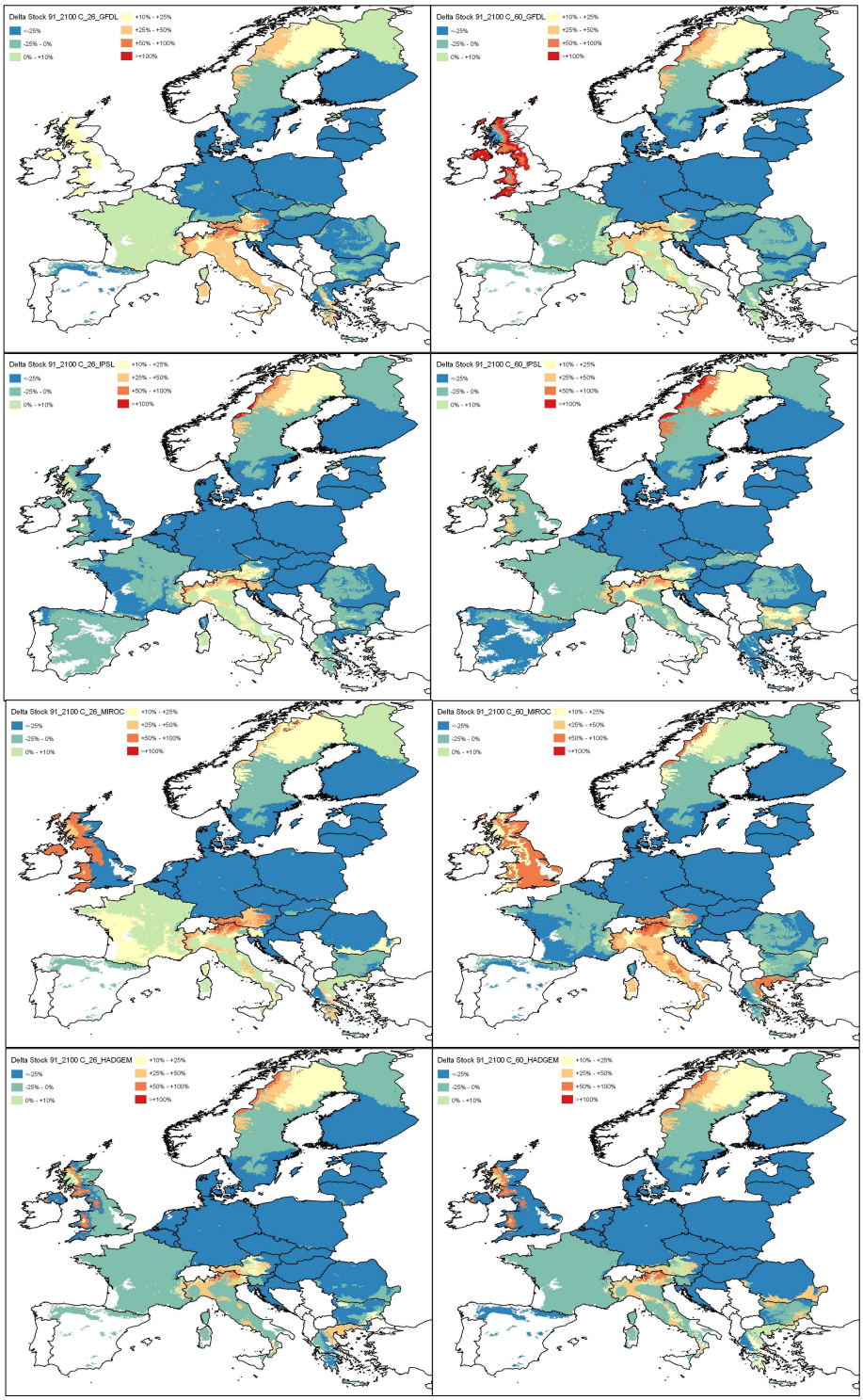

Fig. 5S: relative stock change applied to conifers (reported for the period 2091-2100) as derived from climatic models and used as input for CBM to define the GM. RCP 26 is reported on the left side and RCP 60 on the right side. White areas highlight missing data, not provided from climatic models. Missing data in Ireland were replaced with data from conterminous CLUs from UK and missing data in Portugal with conterminous CLUs in Spain. In this last country, for GFDL, MIROC and HADGEM, some missing data was also replaced with data provided from conterminous CLUs.

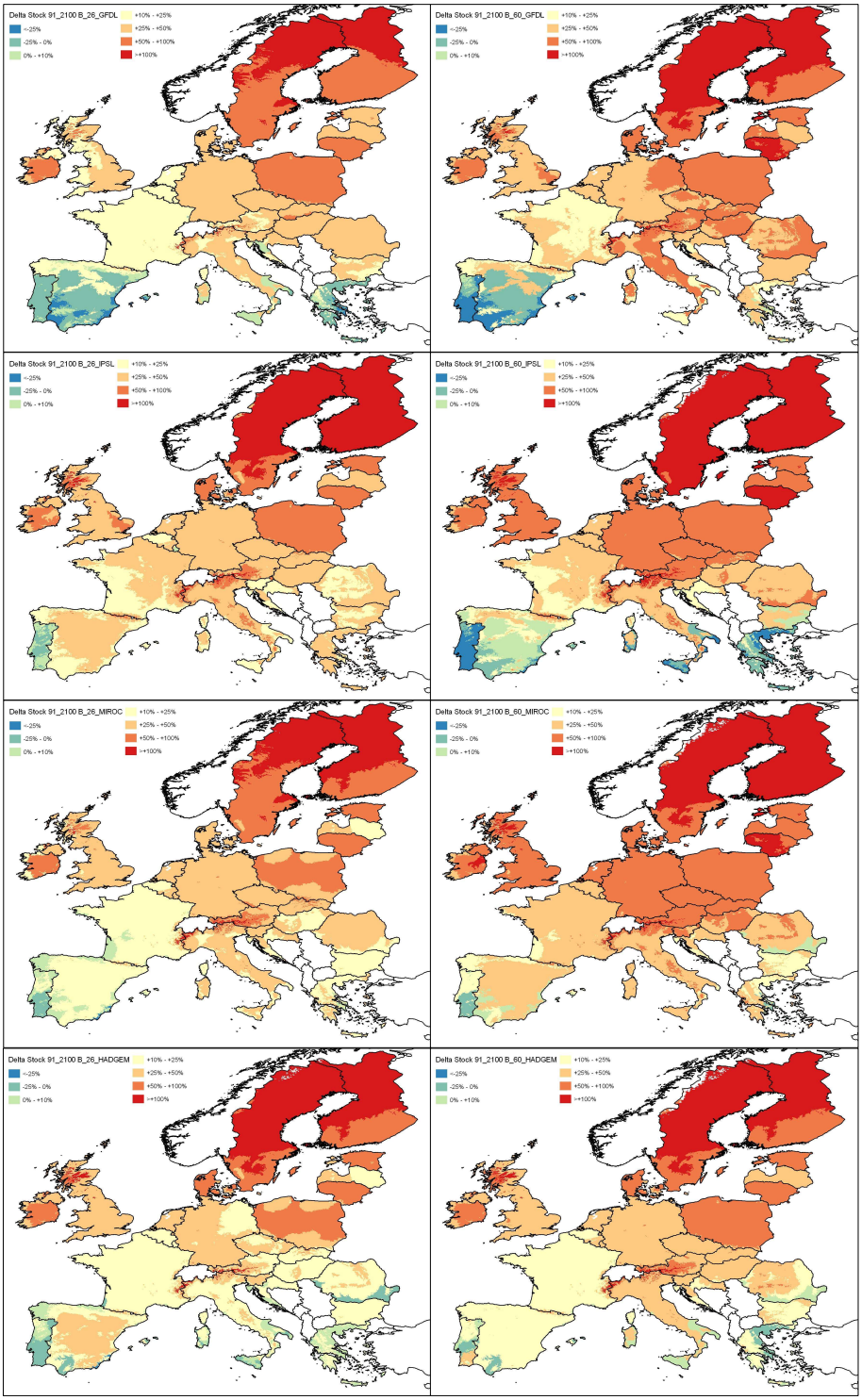

Fig. 6S: relative stock change applied to broadleaved species (reported for the period 2091-2100) as derived from climatic models and used as input for CBM to define the GM. RCP 26 is reported on the left side and RCP 60 on the right side.

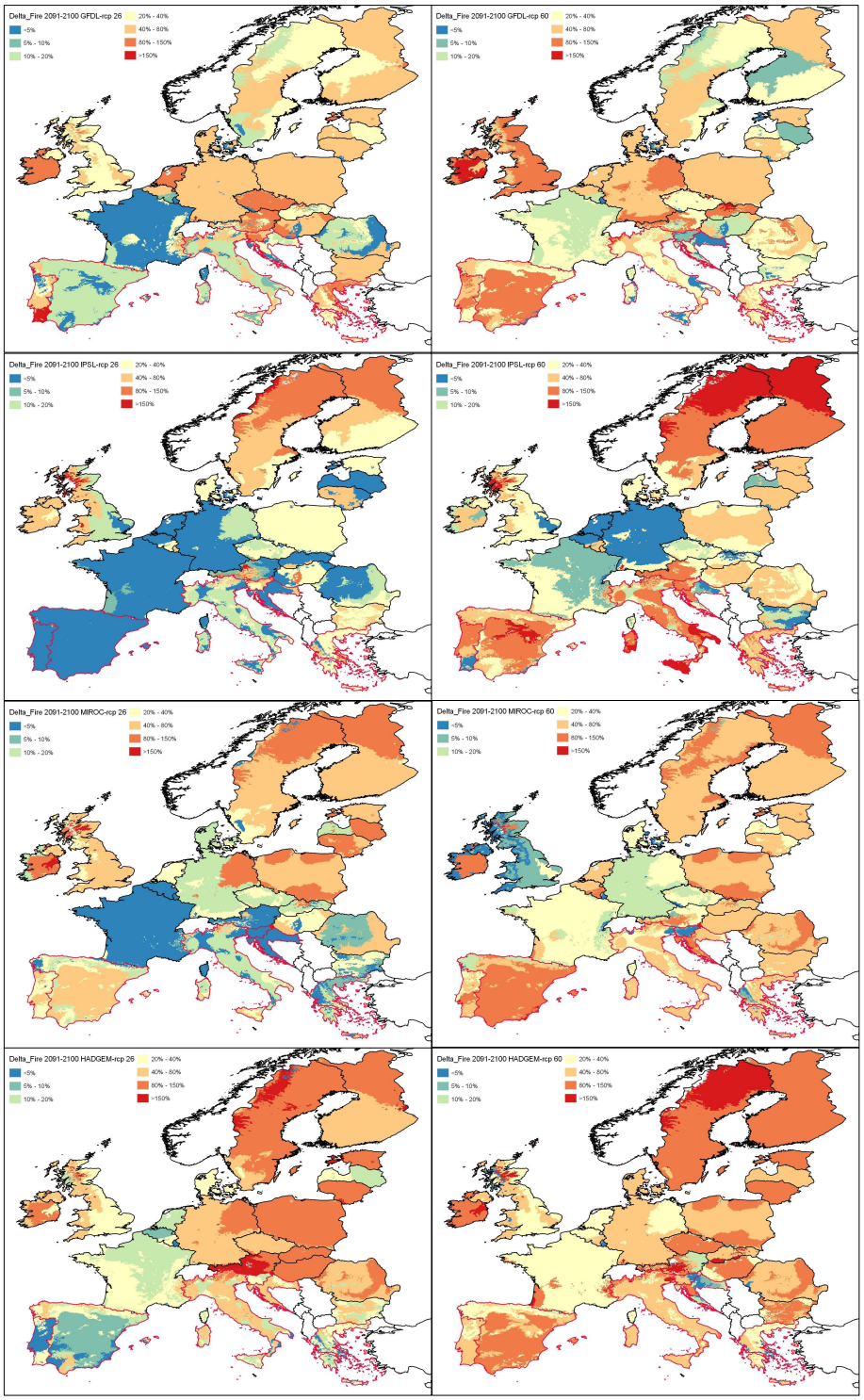

Fig. 7S: relative variation of wildfires frequency for the period 2091-2100, as derived from climatic models and used as input for CBM for 6 Mediterranean countries (highlighted with red outline). RCP 26 is reported on the left side and RCP 60 on the right side.

D. Supplementary materials on model outputs

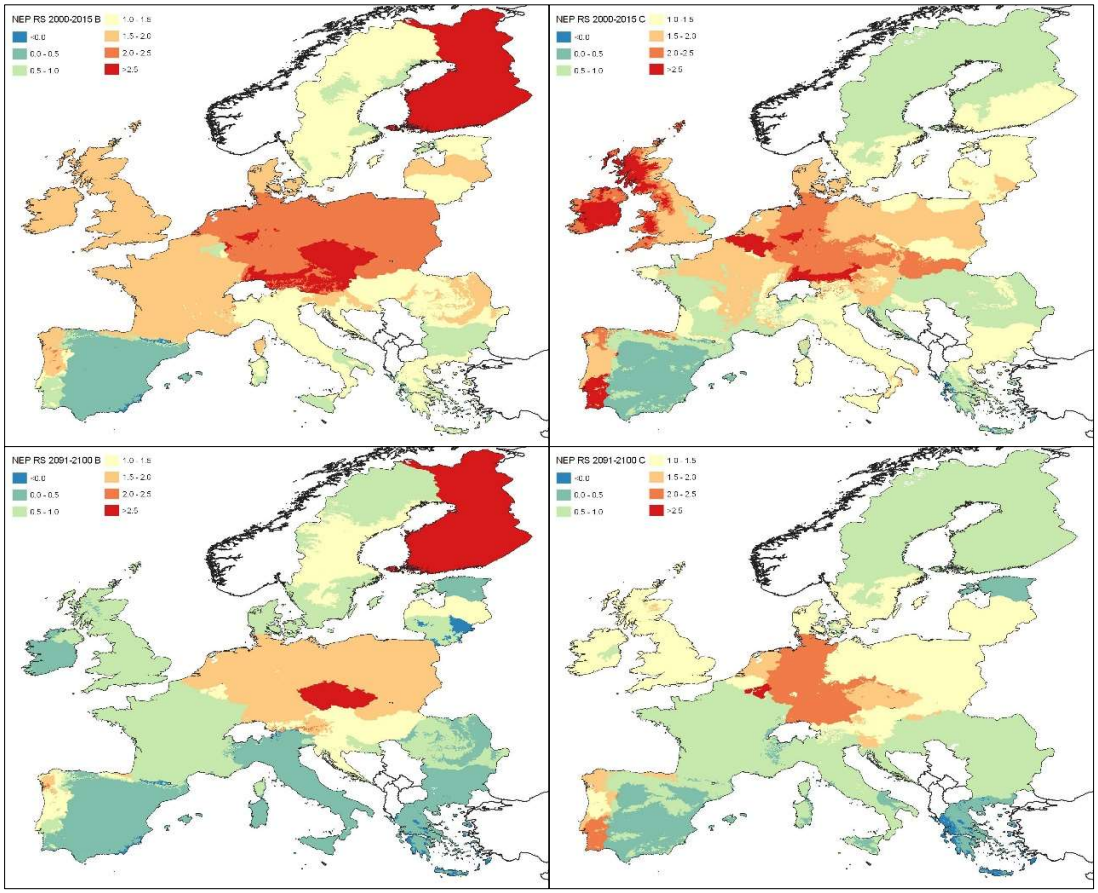

Fig. 8S: geographical distribution of the average Net Ecosystem Production (NEP, in t C ha^{-1} yr^{-1}) estimated by CBM within the historical period 2000 – 2015 and within the decade 2091 -2100 under the RS (i.e., excluding climate change). Broadleaved species are reported on the left side and conifers on the right side.

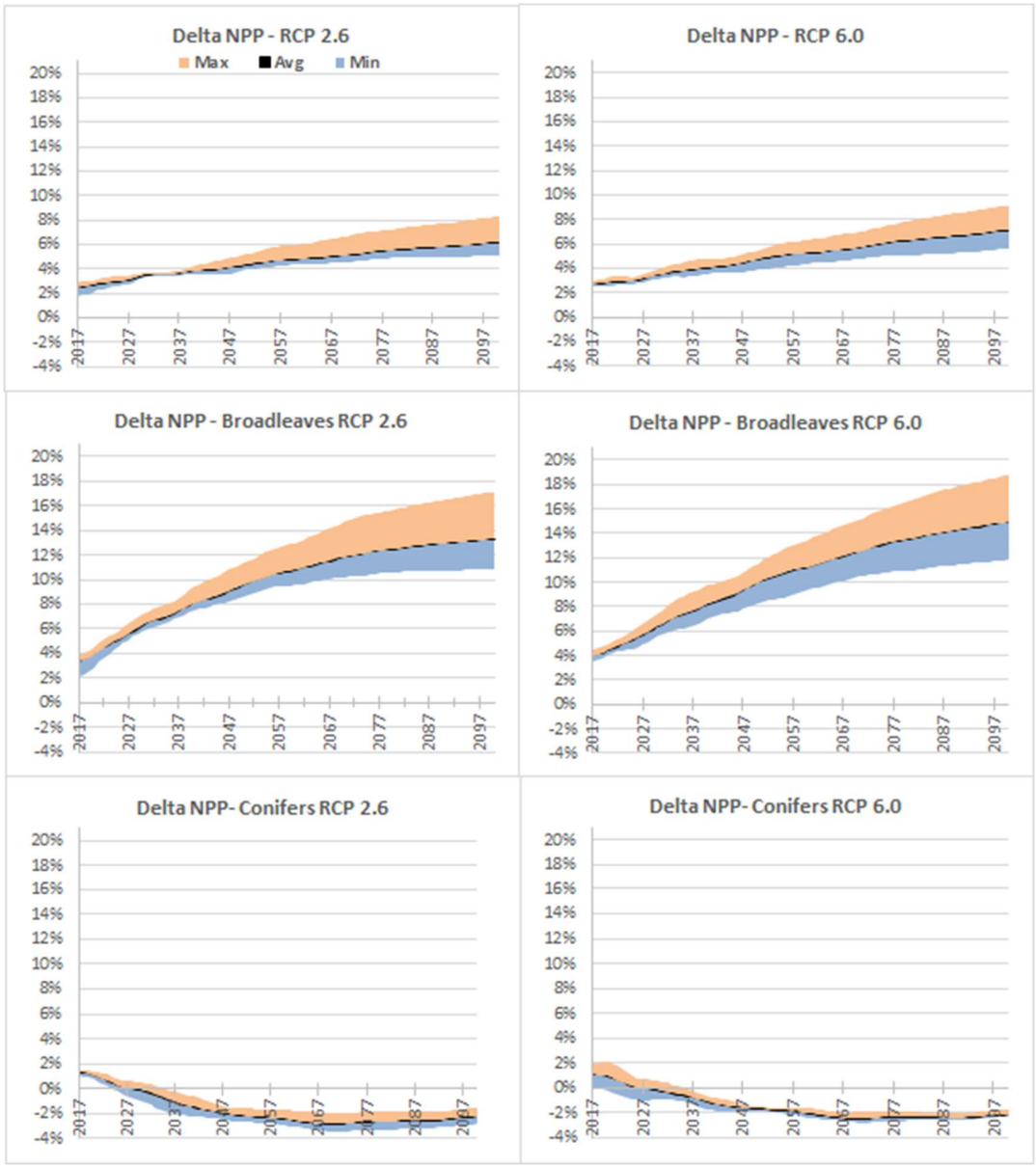

Fig. 9S: average annual rate of variation of the Net Primary Production (NPP), compared to the RS, as derived from the four climate models, at EU level (upper panels), for broadleaved species and for conifers, under different RCP scenarios. Minimum (Min) and maximum (Max) percentage values correspond to the interval between the minimum and maximum difference with the RS for each year. All values are reported as 5-year moving average.

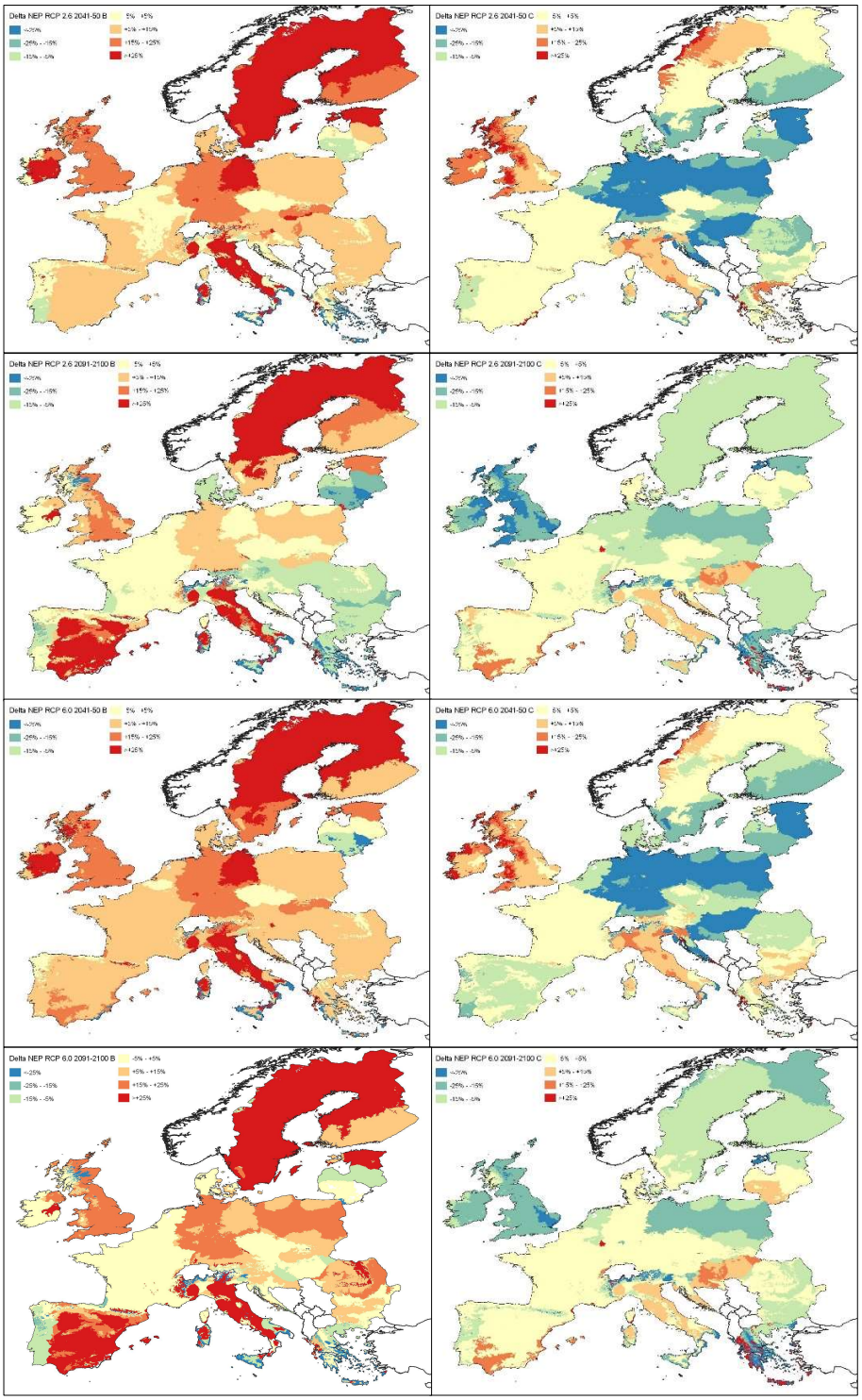

Fig. 10S: relative variation of the NEP due to climate change on broadleaved species (B, on the left side) and conifers (C, on the right side). The relative variation is estimated, for each country and CLU, as average percentage difference between the NEP of the RS and the average NEP estimated from the four climatic models within the periods 2031-2040, 2051-2060, 2071-2080 and 2091-2100. Upper four panels refer to RCP 2.6 and lower four panels to RCP 6.0.

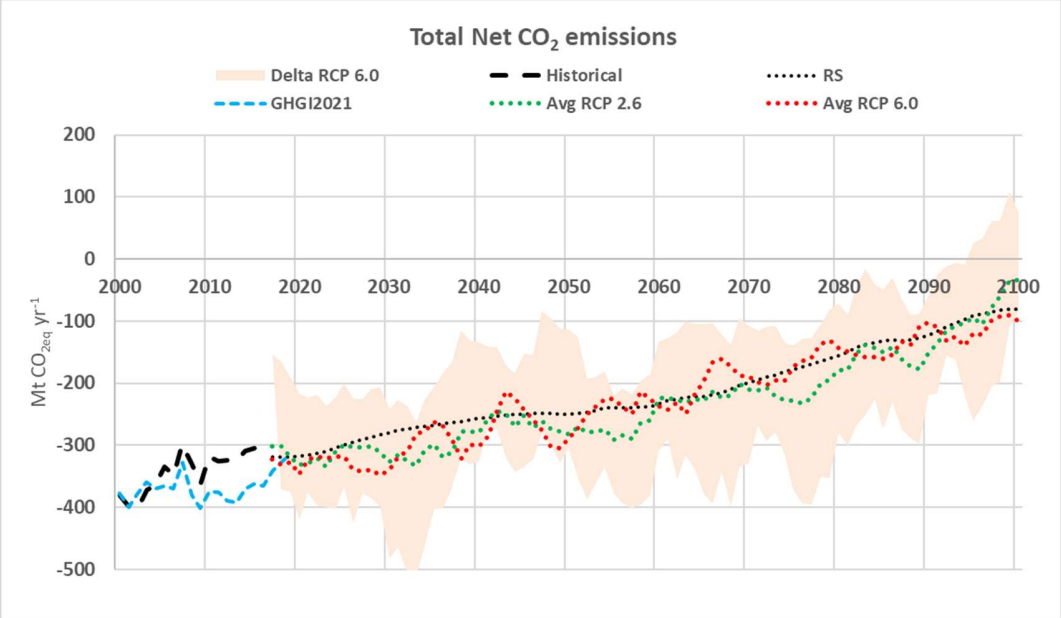

Fig. 11S: total net CO2 emissions (reported as CO2eq. yr-1, with negative values conventionally highlighting CO2 removals from the atmosphere) estimated within the historical period, under the reference scenario (RS), and under RCP 2.6 and RCP 6.0 (reported as the average values estimated from different climate model within each RCP scenario). The figure also reports the net emissions reported from EU27 + UK Member States, according to the Greenhouse Gas Inventory 2021 (GHGI 2021, referred to the category Forest Land Remaining Forest Land, as reported from UNFCCC CRF Tables, 2021), and the range between the minimum and maximum values estimated under RCP 6.0. All values derived from the present study are reported as 5-yrs moving average.

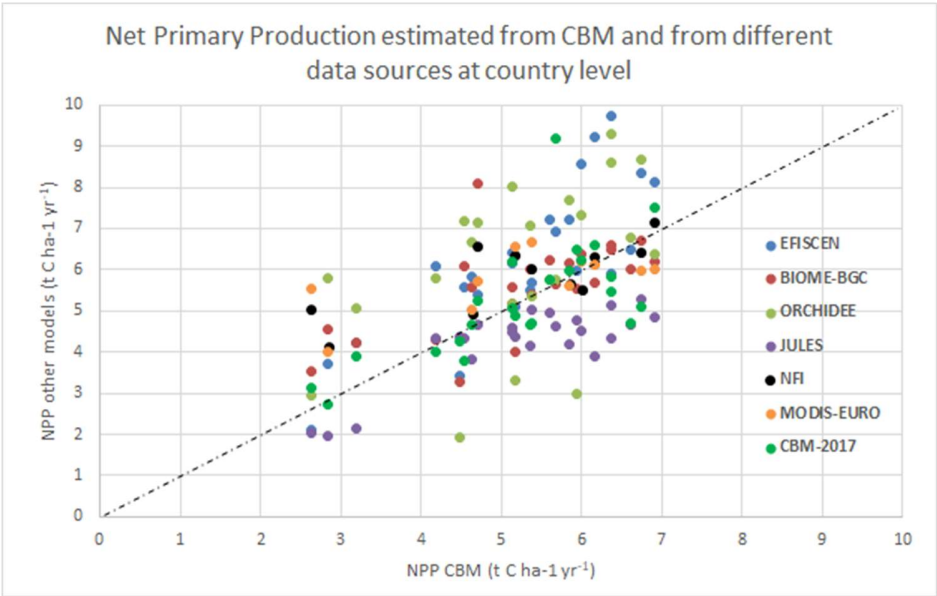

Fig. 12S: comparison between the average Net Primary Production (NPP) estimated by CBM at country level within the historical period 2000 – 2015 in this study, and the corresponding values reported from the following models: EFISCEN (as reported from Tupek et al., 2010), BIOME-BGC (as reported from Tupek et al., 2010), ORCHIDEE (as reported from Tupek et al., 2010), JULES (as

reported from Tupek et al., 2010), NFI data (as reported from Neumann et al., 2016), MODIS-EURO (as reported from Neumann et al., 2016), CBM as applied in Pilli et al. 2017.

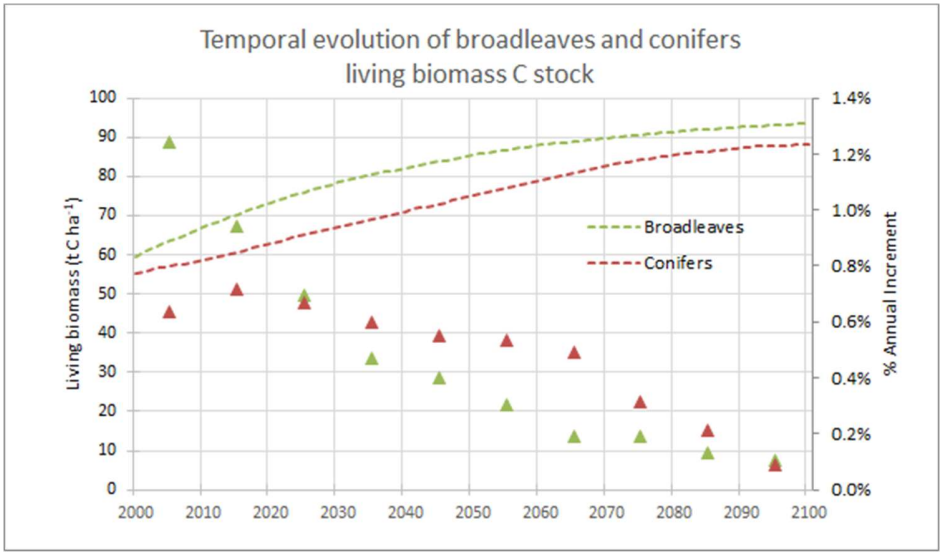

Fig. 13S: temporal evolution of broadleaved species and conifers living biomass C stock (reported in t C ha^{-1} on the left axis), as estimated by CBM within the RS between 2000 and 2100. The right axis reports the evolution of the average percentage annual C stock change estimated on ten years' time intervals.

References

Boudewyn PA, Song X, Magnussen S, Gillis MD (2007) Model-based, volume-to-biomass conversion for forested and vegetated land in Canada. Nat. Resour. Can., Can. For. Serv., Pac. For. Cent., Victoria, BC. Inf. Rep. BC-X-411. [http://cfs.nrcan.gc.ca/publications/?id=27434]

Grassi G; Pilli R. Method applied by the JRC for projecting forest GHG emissions and removals based on the "continuation of current forest management". EUR 28623 EN. Luxembourg (Luxembourg): Publications Office of the European Union; 2017. doi:10.2760/844243

Hijmans, R., Cameron, S.E., Parra, J.L., Jones, P.G., Jarvis, A., 2005. Very high resolution interpolated climate surfaces for global land areas. Int. J. Climatol. 25,1965–1978.

Kull SJ, Rampley G, Morken S, Metsaranta J, Neilson ET, Kurz WA (2016) Operational-scale Carbon Budget Model of the Canadian Forest Sector (CBM-CFS3) version 1.2: user's guide. Nat. Resour. Can., Can. For. Serv., North. For. Cent., Edmonton, AB

Kurz WA, Dymond CC, White TM, Stinson G, Shaw CH, Rampley GJ, Smyth C, Simpson BN, Neilson ET, Trofymow JA, Metsaranta J, Apps MJ (2009) CBM-CFS3: a model of carbon-dynamics in forestry and land-use change implementing IPCC standards. Ecol Model 220(4):480–504. https://doi.org/10.1016/j.ecolmodel.2008.10.018

Li Z, Kurz WA, Apps MJ, Beukema SJ (2003) Belowground biomass dynamics in the Carbon Budget Model of the Canadian Forest Sector: recent improvements and implications for the estimation of NPP and NEP. Can J For Res 33:126–136. https://doi.org/10.1139/X02-165

Motulsky, H.J., Ransnas, L.A., 1987. Fitting curves to data using nonlinear regression: a practical and nonmathematical review. FASEB J. 1, 365–374.

Pilli R (2012) Calibrating CORINE Land Cover 2000 on forest inventories and climatic data: an example for Italy. Int J Appl Earth Obs Geoinf 9:59–71. https://doi.org/10.1186/s13021-015-0016-7

Pilli R, Grassi G, KurzWA, Smyth CE, Blujdea V (2013) Application of the CBM-CFS3 to estimate Italy's forest carbon budget, 1995 to 2020. Ecol Model 266:144–171. https://doi.org/10.1016/j.ecolmodel.2013.07.007

Pilli, R., 2012. Calibrating CORINE Land Cover 2000 on forest inventories and climatic data: an example for Italy. Int. J. Appl. Earth Obs. 9, 59–71.

Pilli, R., Kull, S. J., Blujdea, V. N., & Grassi, G. (2018). The carbon Budget model of the Canadian forest sector (CBM-CFS3): customization of the archive index database for European Union countries. *Annals of forest science*, *75*(3), 1-7.

Sit, V., 1994. Catalog of curves for curve fitting. In: Biometrics Information Handbook Series 4. Ministry of Forest, Victoria, British Columbia (Canada).

Tang, J., Luyssaert, S., Richardson, A. D., Kutsch, W., & Janssens, I. A. (2014). Steeper declines in forest photosynthesis than respiration explain age-driven decreases in forest growth. *Proceedings of the National Academy of Sciences*, *111*(24), 8856-8860.